Universality at Breakdown of Quantum Transport on Complex Networks

Nikolaj Kulvelis, Maxim Dolgushev, and Oliver Mülken*
Physikalisches Institut, Universität Freiburg, Hermann-Herder-Strasse 3, D-79104 Freiburg, Germany
(Received 28 May 2015; published 17 September 2015)

We consider single-particle quantum transport on parametrized complex networks. Based on general arguments regarding the spectrum of the corresponding Hamiltonian, we derive bounds for a measure of the global transport efficiency defined by the time-averaged return probability. For treelike networks, we show analytically that a transition from efficient to inefficient transport occurs depending on the (average) functionality of the nodes of the network. In the infinite system size limit, this transition can be characterized by an exponent which is universal for all treelike networks. Our findings are corroborated by analytic results for specific deterministic networks, dendrimers and Vicsek fractals, and by Monte Carlo simulations of iteratively built scale-free trees.

DOI: 10.1103/PhysRevLett.115.120602 PACS numbers: 05.60.Gg, 05.90.+m, 64.60.aq

Introduction.—Complex networks are intensively used as models for a panoply of physical, chemical, biological, or sociological systems, see [1–3] and references therein. They have been proven to be extremely useful in understanding the statistical as well as the dynamical features of these systems; e.g., the complexity of the structure of the internet is captured by scale-free networks, where the probability distribution of the number of connections of a given node (hub) follows a power law [4]. In contrast to stochastic networks, also deterministic networks—such as regular, hyperbranched, or fractal types—have been applied to study the properties of, say, macromolecular compounds and polymers [5,6].

Networks show a rich statistical behavior, allowing us to study, for instance, critical phenomena [7], entropic properties [8], phase diagrams [9], or the superconductor-insulator transition [10]. Interestingly, many topologically different networks show similar statistical (equilibrium) properties; i.e., they fall into the same universality class [3]. Recently, it has been shown that, in addition to these classes, there are also dynamic universality classes, referring to similar classical diffusive dynamics of different type and on different networks [11]. However, it is by no means clear that a corresponding quantum dynamics on such networks allows for a classification based on a quantum analog of dynamic universality. As will be presented below, one can also define such a quantum analog for (single-particle) quantum transport processes on complex networks. One might encounter such networks over which the dynamics of excitations is (partly) coherent, for instance, in ensembles of LH1 and LH2 complexes in bacterial light-harvesting antennas [12,13], dendritic macromolecules [14,15], or in quantum information theory when studying quantum search algorithms on quantum decision trees [16] or quantum navigation [17] and search engine ranking [18] on complex networks.

In this Letter, we will be concerned with treelike networks. As we show, classes of parametrized Hamiltonians lead to a power-law dependence of a (time-averaged) characteristic quantity describing transport efficiency [19].

Quantum transport efficiency.—We consider systems modeled by undirected networks (graphs) $\mathcal{G}(\mathcal{V},\mathcal{E})$ having a set $\mathcal{V}$ of N nodes and a set $\mathcal{E}$ of bonds. To each node j, we associate a state $|j\rangle$, such that all these states form a basis set of the Hilbert space. The direct couplings between two nodes j and k are mediated by a bond; the number of direct couplings of node j is called functionality (or degree) f_j. The dynamics starting from a localized state $|j\rangle$ is then modeled by Schrödinger's equation ($\hbar \equiv 1$) for the transition amplitudes $\alpha_{k,j}(t) \equiv \langle k|\exp(-i\boldsymbol{H}t)|j\rangle$ [16,19]. We will consider only such Hamiltonians with identical coupling strengths $H_{k,j} \equiv \langle k|\boldsymbol{H}|j\rangle = 1$ between any pair of nodes connected by a single bond and with on-site potentials $H_{j,j} = H(f_j)$; i.e., nodes of the same functionality have the same potential [20].

Based on $\alpha_{k,j}(t)$ and the corresponding transition probabilities $\pi_{k,j}(t) = |\alpha_{k,j}(t)|^2$, we will characterize a network's transport efficiency by the average return values $\bar{\alpha}(t) = (1/N)\sum_{j=1}^{N}\alpha_{jj}(t)$ and $\bar{\pi}(t) = (1/N)\sum_{j=1}^{N}\pi_{jj}(t)$ [19]. Generally, values of $\bar{\pi}(t) = O(1)$ for almost all t imply—on average—a high probability for an excitation to remain at the initial node, thus, indicating inefficient transport, values of $\bar{\pi}(t) \ll 1$ for almost all t suggesting the opposite. Clearly, one needs the entire knowledge of $\boldsymbol{H}$'s eigenspace. For $\bar{\pi}(t)$ this can be circumvented by using the Cauchy-Schwarz inequality to obtain a lower bound [19]

$$|\bar{\alpha}(t)|^2 = \sum_{E,E'} \varrho(E)\varrho(E')e^{-i(E-E')t} \le \bar{\pi}(t), \qquad (1)$$

where $|\bar{\alpha}(t)|^2$ solely depends on the spectral density $\varrho(E)$ of $\boldsymbol{H}$. Asymptotic time-independent measures for the global transport efficiency can be introduced by the return-quantities' infinite time limit

 © 2015 American Physical Society

$$\chi \equiv \lim_{t\to\infty} \frac{1}{t}\int_0^t dt' |\bar{\alpha}(t')|^2 \leq \lim_{t\to\infty} \frac{1}{t}\int_0^t dt' \bar{\pi}(t') \equiv \bar{\chi}. \quad (2)$$

As a lower bound, χ is most instructive if $\chi = O(1)$, thus, the exact value $\bar{\chi}$ is also of order $O(1)$. Then, we regard the global transport as being inefficient, whereas, for $\chi \ll O(1)$, there is no strict implication on $\bar{\chi}$. However, previous results suggest that in particular the maxima of $\bar{\pi}(t)$ are well reproduced by the lower bound $|\bar{\alpha}(t)|^2$, therefore, also indicating that the values of $\bar{\chi}$ lie close to the values of χ [19].

Combining Eqs. (1) and (2) allows us to estimate χ from below, knowing only the spectral density $\varrho(E_*)$ of one arbitrary eigenvalue E_*,

$$\chi = \sum_E \varrho^2(E) \geq \varrho^2(E_*) + \frac{1}{N}[1-\varrho(E_*)] \equiv \underline{\chi}. \quad (3)$$

Here, we assume a completely flat density $\varrho(E)$ on its support aside from E_*. $\underline{\chi}$ allows for a rather accurate estimation of χ if E_* is a single highly degenerated eigenvalue compared to all other eigenvalues, i.e., if $\varrho(E_*) \gg \varrho(E \neq E_*)$, or if all eigenvalues are nondegenerate, i.e., $\rho(E) = 1/N$ for all E. These two limits correspond to vastly different networks: Chainlike networks with $\boldsymbol{H}$ belonging to the above mentioned class have eigenvalues with (mostly) the same degeneracy, i.e., $\rho(E) = \text{const}$ for all E, which yields $\underline{\chi} = \chi = 1/N$ [19], suggesting very efficient transport. In contrast to this, stars of the same size typically have a single highly degenerate eigenvalue yielding $\underline{\chi} = \chi = 1 - (4N-6)/N^2$ [19], thus, rendering transport inefficient. Obviously, in the infinite system size limit, one has $\underline{\chi}_\infty \equiv \lim_{N\to\infty}\underline{\chi}$, which equals zero for chains and one for stars. We note that also regular square and cubic lattices show a similar spectrum as the chain because the eigenvalues follow from a Hamiltonian which is a direct product of two or three one-dimensional chain Hamiltonians, respectively, [19].

Breakdown of quantum transport.—For networks whose spectra depend on a tunable parameter $\sigma \in \mathbb{R}$ such that $\rho(E_*)$ is of order $O(1/N)$ for large values of σ and for small values of σ of order $O(1)$, one might observe a transition from efficient to inefficient transport. Let this transition occur at a given parameter value σ_c. At this value, the transport breaks down which is reflected by a change of $\underline{\chi}(\sigma)$ from values of $O(1/N)$ for $\sigma > \sigma_c$ to values of $O(1)$ for $\sigma < \sigma_c$. Note that, for few or many highly degenerate eigenvalues, χ will be strictly smaller than 1. The complete breakdown is reminiscent of a phase transition where, in our case, the quantity $1 - \underline{\chi}_\infty(\sigma)$ represents the order parameter. (We use the usual terminology of phase transitions in order to stress the similarities and to avoid overloading the Letter with new terminology.) Consequently, we associate with this transition a critical exponent defined by

$$\underline{\kappa} \equiv \lim_{\sigma\to\sigma_c} \frac{\log|1-\underline{\chi}_\infty(\sigma)|}{\log|\sigma-\sigma_c|}. \quad (4)$$

Since $\underline{\chi}_\infty(\sigma) \leq \chi_\infty(\sigma)$, one has $\underline{\kappa} \geq \kappa$, where κ is the exponent associated with the transition for $\chi_\infty(\sigma)$. As we will show below, treelike networks which have a parametrized transition from chainlike topologies to starlike topologies yield the same exponent $\underline{\kappa}$. This allows us to group networks, depending on their asymptotic (global) quantum transport efficiency, into universal classes defined by $\underline{\kappa}$. Our results indicate a continuous (i.e., second or higher order) transition, since there is no discontinuity in the order parameter at the critical point if there remains only a single E_* for σ values in a small neighborhood close to σ_c, which is the case for treelike networks, see below.

Treelike networks.—Figure 1 shows examples of three treelike networks: (a) a scale-free tree (SFT), where the functionalities are drawn from the probability distribution $P(f_j = x) \propto x^{-s}$ (here, $s = 2.5$), (b) a Dendrimer (D) of generation five with functionality $f = 3$, and (c) a Vicsek fractal (VF) of generation three with functionality $f = 4$. For D, the functionality f refers to those nodes having more than one bond, and for VF, it refers to the building blocks of the fractal in each iterative step, see the squares as a guide to the eye in Fig. 1(c). We do not distinguish between the respective functionalities, but we will always note by superscripts D and VF to which structure we refer. D and VF allow for a direct computation of χ and $\underline{\chi}$ based on Eq. (3), since their spectra are exactly known [21–23]. For SFT, one has to resort to either numeric calculations of the spectra or to an analytic estimation of the spectral density of that eigenvalue with the highest degeneracy by counting those nodes (leaves, green triangles in Fig. 1) of the network which only have a single bond. In doing so, we

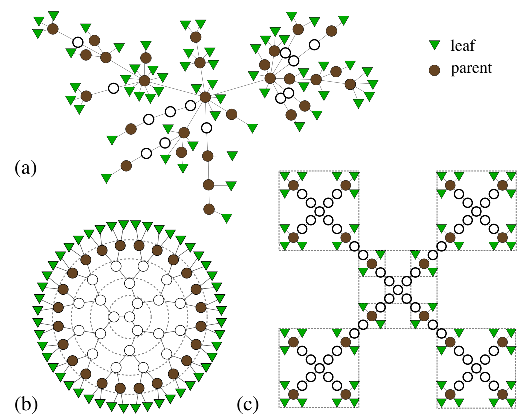

FIG. 1 (color online). Examples of three treelike networks: (a) a scale-free tree, see text for details, (b) a Dendrimer of generation five with functionality $f = 3$, and (c) a Vicsek fractal of generation three with functionality $f = 4$. Three different types of nodes are marked: leaves (green triangles), parents (brown circles), and all other (open circles).

will also need to estimate the number of nodes (parents, brown circles in Fig. 1) to which the leaves are connected, see below.

As is easily shown, if a parent node j has two different leaves l and k, then the superposition state $(|l\rangle - |k\rangle)/\sqrt{2}$ is a normalized eigenstate of the network. The total amount of these superposition states—all belonging to the same eigenvalue $E_* = 1$, regardless their parents because, we have assumed equal couplings in $\boldsymbol{H}$—can be directly calculated. We note, that there could also be other eigenstates, not only involving leaves and parents, leading to the same eigenvalue [23,24]. Since the number of these latter states is small, we concentrate on the former states. Let $N_{L,j}$ be the number of leaves of a single parent j, then there are exactly $N_{L,j} - 1$ independent eigenstates of such a superposition type. Clearly, the more leaves a parent has, the larger will be the number of independent eigenstates for a given eigenvalue, i.e., the larger will be the corresponding spectral density $\varrho(E_*) \geq (N_L - N_P)/N$, where N_L is the number of all leaves and N_P is the number of *all* parents, which, in turn, can be related to N_L: Assuming that a parent j has functionality f_j and that it is also connected to $\delta_j + 1$ nodes which are not leaves, then the number of leaves of this node is $(f_j - \delta_j - 1)$. Let I_P be the index set of all parents, then $N_L = \sum_{j\in I_P}(f_j - \delta_j - 1)$. With $N_P = \sum_{j\in I_P} 1 > 1$, we obtain $N_P = N_L/(\langle f - \delta\rangle_{N_P} - 1)$, where $\langle f - \delta\rangle_{N_P} \equiv \sum_{j\in I_P}(f_j - \delta_j)/N_P$ is the average over the set of all parents. Given the treelike topology, we can estimate N_L based on N and the average functionality of those nodes which are not leaves, $\langle f\rangle_{N\backslash N_L}$: For trees, there are $N - 1$ bonds connecting the N nodes. In the two extreme cases of chains ($\langle f\rangle_{N\backslash N_L} = 2$) and stars ($\langle f\rangle_{N\backslash N_L} = N - 1$), one has 2 and $N - 1$ leaves, respectively. For other trees, the number of leaves $N_L = N - (N-2)/(\langle f\rangle_{N\backslash N_L} - 1) \in [2, N-1]$. We are now in the position of expressing $\varrho(E_*)$ in terms of N and the averaged functionalities $\langle f\rangle_{N_P}$ and $\langle f\rangle_{N\backslash N_L}$. Inserting into the rhs of Eq. (3), one obtains up to order $1/N$

$$\underline{\chi} \geq \left(1 - \frac{1}{\langle f\rangle_{N\backslash N_L} - 1}\right)^2 \left(1 - \frac{1}{\langle f - \delta\rangle_{N_P} - 1}\right)^2 + \frac{1}{N}\left[1 - \left(\frac{\langle f\rangle_{N\backslash N_L} - 2}{\langle f\rangle_{N\backslash N_L} - 1}\right)\left(\frac{\langle f - \delta\rangle_{N_P} - 2}{\langle f - \delta\rangle_{N_P} - 1}\right) + 4\left(\frac{\langle f\rangle_{N\backslash N_L} - 2}{(\langle f\rangle_{N\backslash N_L} - 1)^2}\right)\left(\frac{\langle f - \delta\rangle_{N_P} - 2}{\langle f - \delta\rangle_{N_P} - 1}\right)^2\right]. \quad (5)$$

In the limit when $\langle\delta\rangle_{N_P}/\langle f\rangle_{N_P} \ll 1$, i.e., when a parent is only rarely coupled to more than one other parent, one has $\langle f - \delta\rangle_{N_P} \simeq \langle f\rangle_{N_P}$, where $\langle f\rangle_{N_P}$ can often be written as a function of $\langle f\rangle_{N\backslash N_L}$. If the functionality of nodes which are not leaves does not systematically depend on the position in the network, one has $\langle f\rangle_{N_P} = \langle f\rangle_{N\backslash N_L} \equiv \langle f\rangle$. We note that there are exceptions, see, also, the VF below. Equation (5) defines only a lower bound to $\underline{\chi}$ because we have neglected those eigenstates which are not simple superpositions of two states localized at leaves belonging to the same parent. In the infinite system size limit, these states are negligible close to the transition point, such that the equality holds for $\underline{\chi}_\infty$.

Considering the inverse of the average functionality as the network's adjustable parameter, i.e., $\sigma = 1/\langle f\rangle$, we can deduce a universal behavior at the breakdown of quantum transport. In the limit $N \to \infty$, we obtain

$$\underline{\chi}_\infty = \left(1 - \frac{1}{\langle f\rangle - 1}\right)^4, \quad (6)$$

which results in

$$\underline{\kappa} = \lim_{1/\langle f\rangle \to 0} \frac{\log[1 - \underline{\chi}_\infty]}{\log[1/\langle f\rangle]} = 1, \quad (7)$$

regardless of the original underlying network, be it deterministic or random. Therefore, all treelike networks with a single E_* will yield the same universal exponent $\underline{\kappa}$. We stress, again, that there is no breakdown (for any network, with or without loops) if there is more than one highly degenerate eigenvalue.

Examples.—In order to corroborate our general findings, we consider the three examples of treelike networks depicted in Fig. 1. All these networks allow for a parametrized transition from chainlike to starlike topologies, depending on the (average) functionality. While D and VF allow for a direct computation of χ and $\underline{\chi}$ based on Eq. (3), we will employ Eq. (5) for SFT, which, depending on $\langle f\rangle$, can have many leaves. For normalization purposes, it is inevitable for finite systems to impose a maximal functionality $f_{\max} \leq N - 1$ such that $\langle f\rangle = \Sigma_{f=2}^{f_{\max}} f^{-s+1}/\Sigma_{f=2}^{f_{\max}} f^{-s}$. Inserting this in Eq. (5) yields $\underline{\chi}^{\mathrm{SFT}}$. $\langle f\rangle$ depends on the scaling parameter s, such that $1/\langle f\rangle \to 0$ when $s \searrow 2$. In the limit $N \to \infty$, the averages are related to the Riemann zeta function $\zeta(s) = \Sigma_{f=1}^{\infty} f^{-s}$ allowing us to write the leading terms for values of $s \gtrsim 2$ as

$$\underline{\chi}_\infty^{\mathrm{SFT}} = 1 - 4\frac{\zeta(s) - 1}{\zeta(s-1) - \zeta(s)}. \quad (8)$$

Therefore, the critical exponent follows as

$$\underline{\kappa} = \lim_{s\searrow 2} \frac{\log(1 - \underline{\chi}^{\mathrm{SFT}})}{\log(s-2)} = 1, \quad (9)$$

which, again, confirms our general statement about the universal behavior of treelike networks.

Figure 2 shows the dependence of $1 - \underline{\chi}^{\mathrm{SFT}}$ on the scale-free parameter s and, as inset, on $\langle f\rangle$ for different sizes N and, also, for $N \to \infty$. For finite SFT, we have compared our analytic estimation given by Eq. (5) (lines) with

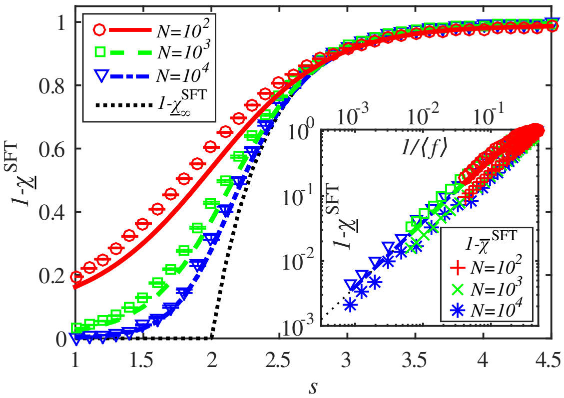

FIG. 2 (color online). Numerical (open symbols) and analytical (lines) results for $1-\underline{\chi}^{\mathrm{SFT}}$: For $N=10^2, 10^3$, and 10^4, the ensemble averages for $1-\underline{\chi}^{\mathrm{SFT}}$ with $R=10^6/N$ realizations are shown (in linear scale) as functions of s. The analytical estimates are obtained from Eq. (5) with $\delta=0$ for finite SFT and, in the limit $N\to\infty$, from Eq. (8). The inset shows the same curves (in log-log scale) as functions of $1/\langle f\rangle$. Both plots show the clear sign of the breakdown of the quantum transport, with the expected linear behavior close to the transition at $s\searrow 2$ or, equivalently, $1/\langle f\rangle\to 0$. In the inset, we also show the Monte Carlo simulation results for the exact value $1-\bar{\chi}^{\mathrm{SFT}}$ (crosses) [25] which shows the same qualitative behavior as $1-\underline{\chi}^{\mathrm{SFT}}$, now being an upper bound.

Monte Carlo simulations (symbols) for SFT grown iteratively by the algorithm given in [26] with the connectivity matrix defining $\boldsymbol{H}$. In the numerical computations, we have considered ensemble averages of $\underline{\chi}^{\mathrm{SFT}}$ with ensemble sizes of $R=10^6/N$. All curves show the expected scaling close to the transition point where $1/\langle f\rangle\to 0$ and $s\searrow 2$, respectively. One notes, from the inset of Fig. 2, that, with increasing N, the finite-size effects become less pronounced, leading eventually to a sharp transition for $s\searrow 2$. In order to strengthen our statements, we also show, in the inset, the corresponding Monte Carlo simulation results for the exact value $1-\bar{\chi}^{\mathrm{SFT}}$ (crosses), see rhs of Eq. (2). The curves lie below the ones for $1-\underline{\chi}^{\mathrm{SFT}}$ (open symbols), which are an upper bound to $1-\bar{\chi}^{\mathrm{SFT}}$. The exact values confirm the breakdown with an exponent of value 1.

For D and VF, the exact knowledge of their spectral densities [21–23] allows us to calculate χ as well as its lower bound $\underline{\chi}$ as functions of the respective functionalities. According to Eq. (3), we get

$$\chi_\infty^{\mathrm{D}}=\left(1-\frac{2}{f}\right)^2 \quad \text{and} \quad \chi_\infty^{\mathrm{VF}}=1\text{–}6\frac{f-1}{f(f+2)-2}, \tag{10}$$

as well as the corresponding lower bounds

$$\underline{\chi}_\infty^{\mathrm{D}}=\left(1-\frac{1}{f-1}\right)^4 \quad \text{and} \quad \underline{\chi}_\infty^{\mathrm{VF}}=\left(1-\frac{4f-5}{f^2-1}\right)^2. \tag{11}$$

In both cases, we find the breakdown of transport in the limit $1/f\to 0$. In order to be comparable to the SFT, we express both, χ_∞^{D} and $\chi_\infty^{\mathrm{VF}}$, as functions of $\langle f\rangle$. For D, $\langle f\rangle_{N\backslash N_L}=f$, which is not the case for VF, where $\langle f\rangle_{N\backslash N_L}=(f+4)/3$ while $\langle f\rangle_{N_P}=f$. Inserting this into Eq. (10), we obtain for $1/\langle f\rangle\to 0$ that $1-\underline{\chi}_\infty^{\mathrm{D}}\sim 1/\langle f\rangle$ and that $1-\underline{\chi}_\infty^{\mathrm{VF}}\sim 1/\langle f\rangle$. Thus, here also, we find the breakdown leading to the (exact) exponent $\kappa=\underline{\kappa}=1$.

Finally, we stress the differences between D and VF on the one hand and SFT on the other hand: For all structures, the transition happens when $1/f\to 0$ or $1/\langle f\rangle\to 0$. However, for D and VF, having fixed deterministic functionalities f, there is no parameter allowing us to study the behavior of χ_∞ beyond the critical point. Moreover, the limit $f\to\infty$ seems rather artificial in the $N\to\infty$ limit since no real system can ever reach this. The situation is different for SFT: Even though $\langle f\rangle$ diverges for scaling parameters $s\leq 2$, it is possible to study the behavior of $\underline{\chi}_\infty^{\mathrm{SFT}}$ in this parameter region. Further, we note that, for finite SFT, one observes the maximal values of $\underline{\chi}^{\mathrm{SFT}}<1$ only in the limit when $s\to 0$.

We anticipate that a similar treatment as presented here might also be feasible for (some) networks with loops. First analytic results for deterministic networks with loops (excluding self-loops) which allow for having a scaling parameter, such as Husimi cacti [27] and complete-graph based recursive networks [28], show a behavior, including the exponent, which is the same as for trees [29].

Conclusions.—We have shown that the breakdown of quantum transport on complex treelike networks shows a universal behavior characterized by a global transport efficiency measure based on the time-averaged return probability. Parametrizing the corresponding Hamiltonian by the (average) functionality of the nodes of the network allows us to derive bounds for this measure, leading, in the infinite system size limit, to a characteristic universal exponent for all treelike networks. While quantum decision trees are, by definition, trees [16], such that our results can be applied to quantum search algorithms on such networks, loops appear in many other systems, as in the real light-harvesting antenna complexes, where coherent energy transfer (at least at short times) is important [12,13].

We thank Alex Blumen and Anastasiia Anishchenko for fruitful discussion and valuable comments. Support from the Deutsche Forschungsgemeinschaft is acknowledged by O. M. (DFG Grant No. MU2925/1-1) and by M. D. (DFG Grants No. BL 142/11-1 and No. GRK 1642/1).

*muelken@physik.uni-freiburg.de

[1] A.-L. Barabási, Science **325**, 412 (2009).
[2] M. Newman, *Networks: An Introduction* (Oxford University Press, New York, 2010).

[3] M. Barthélemy, Phys. Rep. **499**, 1 (2011).
[4] R. Albert, H. Jeong, and A.-L. Barabási, Nature (London) **401**, 130 (1999).
[5] A. A. Gurtovenko and A. Blumen, Adv. Polym. Sci. **182**, 171 (2005).
[6] S. Reuveni, R. Granek, and J. Klafter, Proc. Natl. Acad. Sci. U.S.A. **107**, 13696 (2010).
[7] S. N. Dorogovtsev, A. V. Goltsev, and J. F. Mendes, Rev. Mod. Phys. **80**, 1275 (2008).
[8] K. Anand, G. Bianconi, and S. Severini, Phys. Rev. E **83**, 036109 (2011).
[9] A. Halu, L. Ferretti, A. Vezzani, and G. Bianconi, Europhys. Lett. **99**, 18001 (2012).
[10] G. Bianconi, Phys. Rev. E **85**, 061113 (2012).
[11] B. Barzel and A.-L. Barabási, Nat. Phys. **9**, 673 (2013).
[12] G. D. Scholes, G. R. Fleming, A. Olaya-Castro, and R. van Grondelle, Nat. Chem. **3**, 763 (2011).
[13] R. Hildner, D. Brinks, J. B. Nieder, R. J. Cogdell, and N. F. van Hulst, Science **340**, 1448 (2013).
[14] O. Mülken, V. Bierbaum, and A. Blumen, J. Chem. Phys. **124**, 124905 (2006).
[15] I. Akai, K. Miyanari, T. Shimamoto, A. Fujii, H. Nakao, A. Okada, K. Kanemoto, T. Karasawa, H. Hashimoto, A. Ishida *et al.*, New J. Phys. **10**, 125024 (2008).
[16] E. Farhi and S. Gutmann, Phys. Rev. A **58**, 915 (1998).
[17] E. Sánchez-Burillo, J. Duch, J. Gómez-Gardeñes, and D. Zueco, Sci. Rep. **2**, 605 (2012).
[18] S. Garnerone, P. Zanardi, and D. A. Lidar, Phys. Rev. Lett. **108**, 230506 (2012).
[19] O. Mülken and A. Blumen, Phys. Rep. **502**, 37 (2011).
[20] Matrices typically associated with graphs $\mathcal{G}$, like its connectivity matrix $[H(f_j) = f_j]$ and its adjacency matrix $[H(f_j) = 0$ for all $j]$, are contained in this class.
[21] C. Cai and Z. Y. Chen, Macromolecules **30**, 5104 (1997); Y. Y. Gotlib and D. A. Markelov, Polym. Sci., Ser. A **44**, 1341 (2002).
[22] C. S. Jayanthi and S. Y. Wu, Phys. Rev. B **50**, 897 (1994).
[23] A. Blumen, C. von Ferber, A. Jurjiu, and T. Koslowski, Macromolecules **37**, 638 (2004).
[24] F. Fürstenberg, M. Dolgushev, and A. Blumen, J. Chem. Phys. **138**, 034904 (2013).
[25] For computational reasons, we chose $R = 10^5/N$ for $N = 10^4$, while we kept $R = 10^6/N$ for smaller values of N.
[26] M. Galiceanu, Phys. Rev. E **86**, 041803 (2012).
[27] M. Galiceanu, J. Phys. A **43**, 305002 (2010).
[28] H. Liu, M. Dolgushev, Y. Qi, and Z. Zhang, Sci. Rep. **5**, 9024 (2015).
[29] See Supplemental Material at http://link.aps.org/supplemental/10.1103/PhysRevLett.115.120602 for the calculations of quantum transport properties for several networks with loops.